

See discussions, stats, and author profiles for this publication at: <https://www.researchgate.net/publication/231396015>

Radical reactions in a single crystal of phosphalkene: EPR and ab initio calculations of phosphoniumyl radical cations

ARTICLE *in* THE JOURNAL OF PHYSICAL CHEMISTRY · OCTOBER 1995

Impact Factor: 2.78 · DOI: 10.1021/j100043a026

CITATIONS

4

READS

16

4 AUTHORS, INCLUDING:



Theo Berclaz

University of Geneva

55 PUBLICATIONS 548 CITATIONS

SEE PROFILE



Michel Geoffroy

University of Geneva

207 PUBLICATIONS 2,136 CITATIONS

SEE PROFILE

Radical Reactions in a Single Crystal of Phosphaalkene: EPR and *ab Initio* Calculations of Phosphoniumyl Radical Cations

Shrinivasa N. Bhat, Théo Berclaz, Michel Geoffroy,* and Abdelaziz Jouaiti

Department of Physical Chemistry, University of Geneva, 30 Quai Ernest Ansermet, 1211 Geneva, Switzerland

Received: June 16, 1995; In Final Form: August 15, 1995*

Two radiogenic radicals trapped in a single crystal of 1-[2,4,6-tri-*tert*-butylphenyl]-2-phenylphosphaethene have been studied by EPR and have been identified, from their ^{31}P hyperfine tensors, as being phosphoniumyl radical cations. The spectra modifications caused by ^{13}C or ^2D enrichment of the phosphaalkene moiety show that these species result from an intramolecular cyclization which can lead to two possible conformations of the radical. The experimental ^{31}P , ^{13}C , and ^1H hyperfine tensors are compared with those predicted by *ab initio* calculations on model phosphoniumyl radical cations. These calculations show that these interactions are very sensitive to the geometry of the radical and that their measurement can yield precise structural information.

Introduction

Dicoordinated trivalent phosphorus compounds are very reactive species which can be stabilized by binding the phosphorus atom to a bulky substituent^{1,2} (e.g., tri-*tert*-butyl). In the case of diphosphene^{3,4} it was shown that the $\text{P}=\text{P}$ moiety rapidly reacts with radicals to produce phosphinyl radicals ($\text{R}_2\text{P}^\bullet$) and more recently we could demonstrate, from solid-state EPR studies, that this mechanism occurs as well for the $\text{P}=\text{C}$ fragment.⁵ In the present paper, we report another radical process involving the phosphaalkene group and show that, under radiolysis, the $-\text{P}=\text{C}-$ bond can give rise to a phosphoniumyl radical cation ($\text{R}_3\text{P}^{+\bullet}$).

In the literature, information about the structure of phosphoniumyl radicals was mainly provided by the analysis of the corresponding ^{31}P hyperfine interaction⁶ and, for example, Tordo et al.⁷ have recently studied the role of the nature of R on the geometry of $\text{R}_3\text{P}^{+\bullet}$ and have pointed out the influence of steric factors. As will be shown below, in addition to its interest in the context of radiation chemistry, the trapping of a phosphoniumyl radical in an X-irradiated single crystal of $\text{ArP}=\text{C}(\text{H})\text{R}'$ [Ar: $\text{C}_6\text{H}_3(\text{tBu})_3$], ^{13}C -1, also offers the possibility of measuring the hyperfine tensors with the ^{31}P nucleus, the ^{13}C located in α -position to the phosphorus atom and a β -proton. These results will be discussed in the light of *ab initio* calculations performed on $(\text{R}_2\text{P}^{13}\text{CH}_3)^{+\bullet}$ species, and special attention will be given to the structural dependence of the calculated coupling constants.

Experimental Section

1-[2,4,6-Tri-*tert*-butylphenyl]-2-phenylphosphaethene, **1** (Chart 1), was synthesized following the method given by Yoshifuji.⁸ The (*E*) isomer was obtained after separation on a silica-gel column. The deuterated compound ^2D -1 [$\text{ArP}=\text{C}(^2\text{D})\text{C}_6\text{D}_5$] and the ^{13}C -enriched compound ^{13}C -1 [$\text{ArP}=\text{C}(\text{H})\text{C}_6\text{H}_5$] were prepared by using as reagent $\text{C}_6\text{D}_5\text{C}(\text{D})\text{O}$ and $\text{C}_6\text{H}_5^{13}\text{C}(\text{H})\text{O}$, respectively. The crystal structure was determined by Appel et al.⁹ monoclinic, $\text{C}2/c$, $a = 41.7$, $b = 5.95$, $c = 18.68$ Å, $\beta = 98.52^\circ$.

The crystals studied by EPR were obtained at -8°C by slow evaporation of a solution of **1** in a mixture $\text{MeCN}/\text{Et}_2\text{O}$. The EPR reference axes were chosen after indexation of the crystal faces: x , y , z were aligned along c , a^* , b , respectively. The

crystals were exposed for 2 h to the radiation of a Philips X-ray tube equipped with a tungsten anticathode (30 kV, 30 mA, room temperature). The EPR spectra were recorded on a Bruker E-200D spectrometer. The angular variation of the signals was obtained by rotating the crystal in steps of 10° around each reference axis. The resulting curves were analyzed with a Hamiltonian which takes the electronic Zeeman interaction as well as the hyperfine couplings with several nuclei¹⁰ into account. The various tensor elements were obtained with an optimization program which compares the positions of the observed signals with those calculated by second-order perturbation.

The *ab initio* calculations were carried out on a Silicon Graphics workstation by using the *Gaussian 90* and *Gaussian 92* programs.^{11,12} The geometries of the phosphoniumyl radicals were optimized by using the UHF method with the 6-31G* basis set. The coupling constants were calculated using the 6-311G** basis set after annihilation of the spin contamination.

Results

Electron Paramagnetic Resonance. An example of an EPR spectrum obtained with an X-irradiated single crystal of **1** is shown in Figure 1. The signals marked B and C have previously been identified⁵ as being due to phosphinyl- and carbon-centered radicals, and here we will be concerned with the signals A which exhibit a large ^{31}P hyperfine splitting (see Figure 1a). In the symmetry plane (a^*c) the various orientations of an identical species are magnetically equivalent and the corresponding curves shown in Figure 2 (top) indicate that each set of lines A probably results from the trapping of two different species (A1 and A2). The curves obtained in the two other planes are consistent with this hypothesis: both A1 and A2 species are characterized by a hyperfine interaction with a ^{31}P and a ^1H nucleus. The simplicity of the spectrum shown in Figure 1a is due to the fact that along this orientation of the magnetic field both species A1 and A2 exhibit the same phosphorus splitting (35.4 mT) and have the same proton coupling (1.5 mT). These results were confirmed by studying the deuterated compound ^2D -1: as shown in Figure 1b, the doublet (splitting = 1.5 mT) observed with the non-deuterated compound is now replaced by three equally spaced lines (splitting = 0.75 mT). Moreover the angular variation (Figure 2, middle) clearly shows that deuteration does not affect the spectrum of radical A1 while it leads

* Abstract published in *Advance ACS Abstracts*, October 1, 1995.

CHART 1

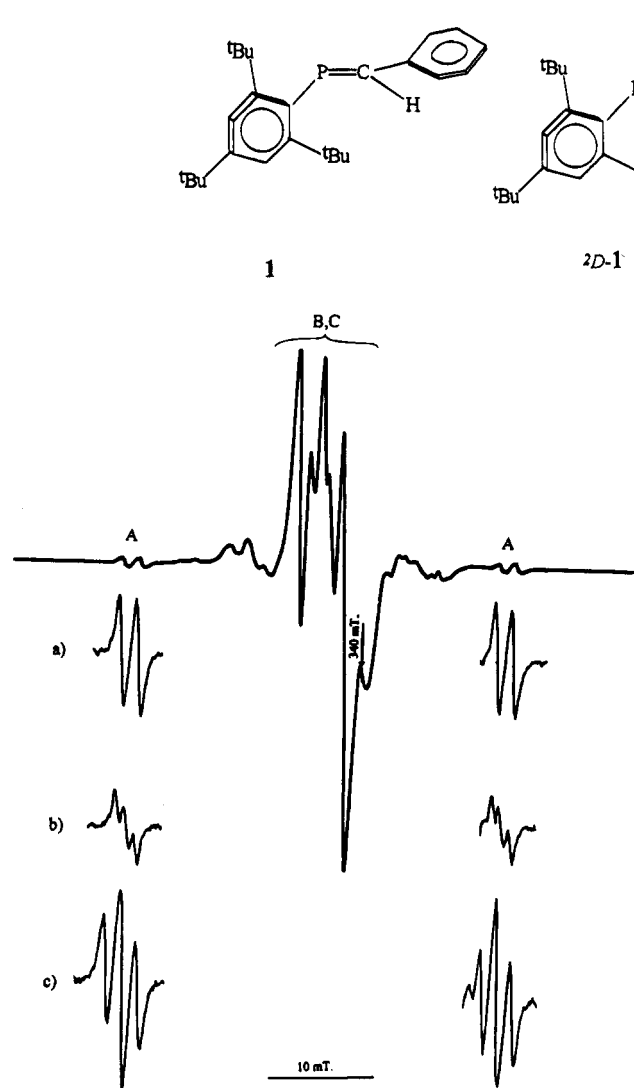


Figure 1. Example of an EPR spectrum obtained with an X-irradiated single crystal of **1** (the magnetic field lies in the a^*c plane, 30° from the $-a^*$ axis). Signals A, recorded with higher gain for this same orientation of the magnetic field, are shown in (a) crystal of **1**, (b) crystal of **²D-1**, and (c) (crystal of **¹³C-1**).

to the suppression of the ^1H splitting of radical A2. Enrichment in ^{13}C has a drastic effect on the spectrum: the doublet of 1.5 mT observed with a crystal of **1** (Figure 1a) is replaced, with a crystal of **¹³C-1**, by a triplet of 1.5 mT (Figure 1c). As shown by the angular variation of the spectra (Figure 3, bottom), both radicals A1 and A2 exhibit now hyperfine couplings with three spin- $1/2$ nuclei (^{31}P , ^1H , ^{13}C). To summarize, the analysis of all the angular variations obtained with the crystals of **1**, **²D-1**, and **¹³C-1** showed that (1) the g , ^1H , and ^{31}P hyperfine tensors obtained for the species A1 were independent of the isotopic enrichment of the precursor and (2) whereas the g and ^{31}P coupling tensors measured for the radical A2 were also independent of the isotopic enrichment; the ^1H hyperfine interaction was not observed, for A2, with a crystal of **²D-1**; the same ^1H tensor was obtained, for A2, with a crystal of **¹³C-1** and with a crystal of **1**. The various EPR tensors for species A1 and A2 are given in Tables 1 and 2 respectively.

Calculations. Some ab initio calculations have been published on phosphoniumyl radical cations,^{13–15} in particular accurate theoretical predictions have been recently obtained¹⁶ for $(\text{CH}_3)_3\text{P}^{++}$ by using the UHF/6-31G** basis set for the geometry optimization and the 6-311G** basis set for the

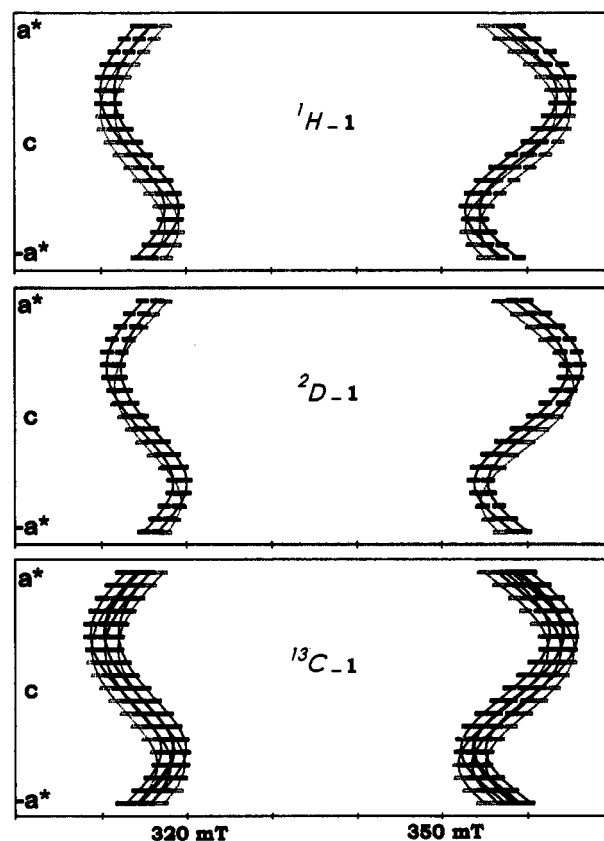


Figure 2. Angular variation of the EPR signals A1 (—) and A2 (···) in the a^*c plane observed with an X-irradiated single crystal of **1** (top), **²D-1** (middle), and **¹³C-1** (bottom).

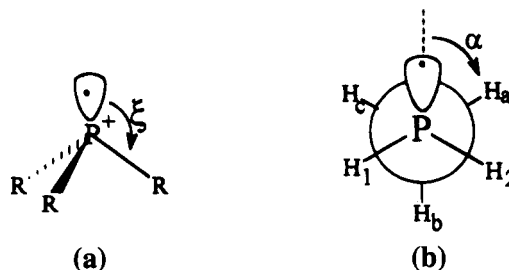


Figure 3. Definitions of the pyramidity angle ξ (a) and of the dihedral angle α (b).

calculation of the coupling constants. Here we are mainly interested in the dependence of the coupling constants on the conformation of the radical cation; in general, we have therefore imposed one structural constraint and optimized all the remaining geometrical parameters by using the 6-31G* basis set, then the various coupling constants were calculated with the 6-311G** basis set. So, to visualize the geometry dependence of the hyperfine couplings for a R_3P^{++} species, we have optimized the structure of H_3P^{++} and $(^{13}\text{CH}_3)_3\text{P}^{++}$ by maintaining C_{3v}

TABLE 1: g and Hyperfine (MHz) Tensors for the Radical A_1

tensor	eigenvalues	λ (/a)	μ (/b)	ν (/c*)
g tensor				
g_1	2.0017	0.2641	∓ 0.6832	0.6808
g_2	2.0048	0.1860	± 0.7287	0.6591
g_3	2.0078	-0.9464	∓ 0.0475	0.3195
^{31}P coupling				
T_1	981	-0.6478	∓ 0.7616	0.0167
T_2	996	-0.6716	± 0.5814	0.4594
T_3	1535	0.3596	∓ 0.2864	0.8881
$^1\text{H}_a$ coupling				
T_1	41	0.7920	± 0.3257	0.5164
T_2	45	0.3274	∓ 0.9405	0.0910
T_3	47	-0.5153	∓ 0.0970	0.8514
^{13}C coupling				
T_1	42	0.0930	± 0.2739	0.9572
T_2	46	-0.9782	∓ 0.1542	0.1392
T_3	49	0.1857	∓ 0.9493	0.2535

TABLE 2: g and Hyperfine (MHz) Tensors for the Radical A_2

tensor	eigenvalues	λ (/a)	μ (/b)	ν (/c*)
g tensor				
g_1	2.0013	0.3908	∓ 0.5938	0.7034
g_2	2.0047	0.4555	± 0.7888	0.4127
g_3	2.0064	-0.7999	± 0.1590	0.5787
^{31}P coupling				
T_1	984	-0.7892	± 0.1905	0.5839
T_2	992	0.3002	± 0.9490	0.0960
T_3	1534	0.5358	∓ 0.2511	0.8062
$^1\text{H}_a$ coupling				
T_1	35	-0.9891	∓ 0.1471	0.0112
T_2	44	-0.1023	± 0.7380	0.6671
T_3	48	0.1064	∓ 0.6586	0.7449
^{13}C coupling				
T_1	42	-0.5135	± 0.2222	0.8288
T_2	48	0.8340	± 0.3565	0.4211
T_3	51	0.2020	∓ 0.9075	0.3684

symmetry and have calculated the Fermi (A_{iso}) and dipolar (τ) hyperfine interactions as a function of the pyramidity angle ξ (Figure 3a).

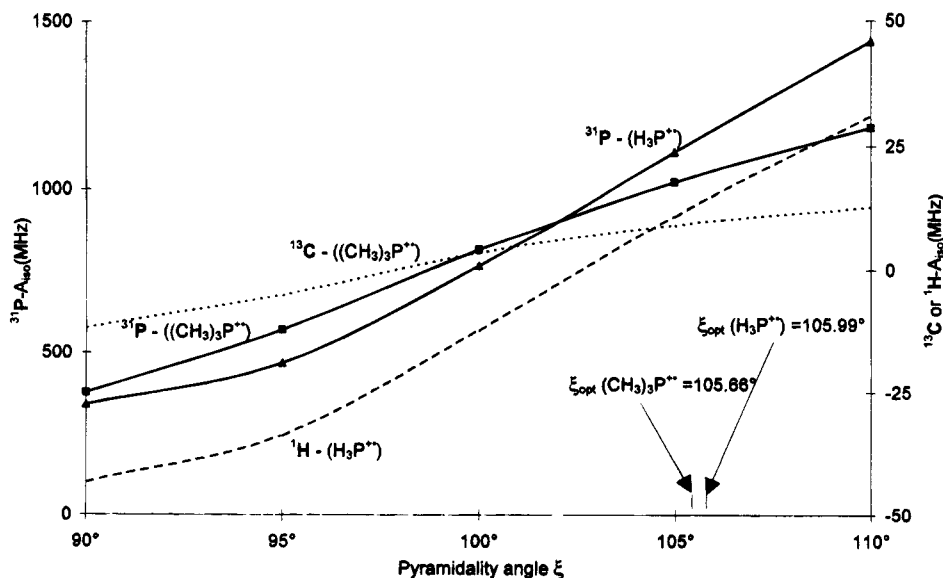
The variations of A_{iso} and τ_{\parallel} calculated when the geometry of these radicals passes from planar ($\xi = 90^\circ$) to tetrahedral ($\xi \sim 110^\circ$) are shown in Figure 4 and Table 3, respectively. The equilibrium structure is found at $\xi = 105.9^\circ$ and at $\xi = 105.6^\circ$ for H_3P^{++} and $(\text{CH}_3)_3\text{P}^{++}$, respectively. For this latter species

TABLE 3: Variation of Dipolar Coupling constants τ_{\parallel} (MHz) for R_3P^{++} with the Pyramidity Angle ξ

angle ξ (deg)	H_3P^{++}		$(\text{CH}_3)_3\text{P}^{++}$	
	$^{31}\text{P}-\tau_{\parallel}$	$^1\text{H}-\tau_{\parallel}$	$^{31}\text{P}-\tau_{\parallel}$	$^{13}\text{C}-\tau_{\parallel}$
90.0	651.2	16.3	632.5	2.7
95.0	640.9	16.2	605.2	3.9
100.0	617.8	15.9	573.3	5.6
105.0	593.1	15.4	550.4	7.2
110.0	571.3	15.0	534.8	8.6

the ^{31}P isotropic coupling constant agrees with the value recently published by Cramer and Lim¹⁶ and both the isotropic and anisotropic couplings ($A_{\text{iso}} = 1043$ MHz, $\tau_{\parallel} = 548$ MHz) are in good accord with the experimental values reported by Symons and McConnachie¹⁷ ($A_{\text{iso}} = 1078$ MHz, $\tau_{\parallel} = 557$ MHz). For $\text{H}_2\text{P}^{++}\text{CH}_3$ we have calculated the dependence of the energy as a function of the dihedral angle α formed by a C—H bond—say C—H_a—and the bisector of the $\text{H}_{(1)}\text{PH}_{(2)}$ angle (Figure 3b). For each value of α the PH and PC bond lengths as well as the HPC angles were optimized by maintaining the distances $\text{H}_{(1)}-\text{P}$ and $\text{H}_{(2)}-\text{P}$ equal and by assuming that the angle $\text{H}_{(1)}\text{PC}$ is equal to the angle $\text{H}_{(2)}\text{PC}$. The resulting curves are shown in Figure 5. As shown by its bond angles ($\text{HPC} = 114.6^\circ$, $\text{HPH} = 109.6^\circ$), the equilibrium geometry of $\text{H}_2\text{P}^{++}\text{CH}_3$ is quite pyramidal and the corresponding ^{31}P coupling constants, equal to $A_{\text{iso}} = 1103$ MHz and $\tau_{\parallel} = 573$ MHz, are slightly larger than those previously obtained with a 3-21G* basis set.¹⁵ The calculations that we have performed on $\text{PhP}^{++}(\text{CH}_3)_2$ (Ph: phenyl group; bond angles at the equilibrium geometry: $\text{Ph}-\text{P}-\text{CH}_3 = 114.7^\circ$, $\text{CH}_3-\text{P}-\text{CH}_3 = 111.6^\circ$), show that the phosphorus couplings are rather sensitive to the replacement of a methyl group by a phenyl ring in $(\text{CH}_3)_3\text{P}^{++}$ since this replacement causes a decrease of 96.8 MHz in $^{31}\text{P}-A_{\text{iso}}$ and of 57 MHz in $^{31}\text{P}-\tau_{\parallel}$.

We have selected the radical cation **2** to model the radiogenic species trapped in a crystal of **1**: the hyperfine constants calculated after optimization of this phosphoniumyl species ($\text{C}=\text{C}$: 1.353 Å, $\text{P}-\text{C}=\text{C}$: 109.3° , $\text{C}-\text{C}=\text{C}$: 118.1°) are shown in Table 4. To estimate the sensitivity of these coupling constants to the geometry of the ring, we have optimized the structure of **2** after having imposed the length of the C=C bond (1.4 Å) and the $\text{P}-\text{C}=\text{C}$ and $\text{C}=\text{C}-\text{C}$ bond angles (115° and 120° , respectively): the resulting coupling constants are also given in Table 4.

**Figure 4.** Variation of the isotropic ^{31}P , ^{13}C , and ^1H coupling constants, for H_3P^{++} and $(\text{CH}_3)_3\text{P}^{++}$ as a function of the pyramidity angle ξ .

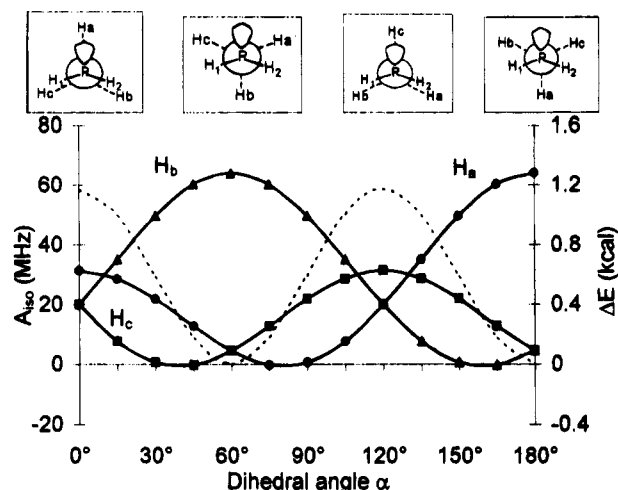
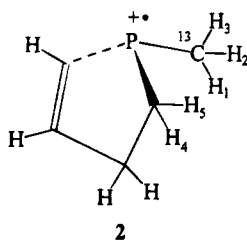


Figure 5. Variation of the calculated methyl proton isotropic coupling constants and of the energy difference ΔE as a function of the dihedral angle α for $\text{H}_2\text{P}^+\text{CH}_3$ (ΔE is calculated by taking the energy of the fully optimized molecule as equal to zero).

TABLE 4: Calculated ESR Coupling Constants^a for the Radical 2

nucleus	isotropic coupling constant A_{iso} (MHz)	anisotropic coupling constants (MHz)		
		τ_i	τ_j	τ_k
^{31}P	925 (961)	453 (417)	-222 (-202)	-231 (-214)
$^1\text{H}_{(1)}$	47 (44)	5 (4)	0 (0)	-5 (-4)
$^1\text{H}_{(2)}$	2 (0)	8 (8)	-3 (-3)	-5 (-5)
$^1\text{H}_{(3)}$	1 (-1)	7 (7)	-2 (-2)	-5 (-5)
^{13}C	18 (22)	9 (10)	-4 (-5)	-5 (-5)
$^1\text{H}_{(4)}$	12 (8)	7 (7)	-3 (-3)	-4 (-4)
$^1\text{H}_{(5)}$	33 (18)	4 (4)	-1 (-1)	-3 (-3)

^a Values in parentheses have been calculated after a small modification of the geometry of **2** (see text).



We have optimized the geometry of PO_3^{2-} assuming a C_{3v} symmetry; the resulting structure is characterized by P—O distances equal to 1.531 Å and by a pyramidity angle ξ equal to 103.7°. The calculated ^{31}P — A_{iso} and ^{31}P — τ_{\parallel} coupling constants are equal to 1185 and 262 MHz, respectively. The calculated charge on the phosphorus atom is equal to +0.935 while the charge on each oxygen atom is equal to -0.978.

Discussion

The ^{31}P , ^1H , and ^{13}C hyperfine tensors obtained for radicals A1 and A2 were decomposed into isotropic and anisotropic coupling constants by assuming that all the eigenvalues of the tensors have the same sign. The resulting values are given in Table 5. The ^{31}P constants indicate that A1 and A2 are very similar species that are characterized by rather large Fermi and dipolar interactions. By assuming positive eigenvalues and by comparing these interactions with those associated to atomic phosphorus,¹⁸ it is found that the spin densities in the 3s and 3p phosphorus orbitals are equal to ~0.09 and ~0.50, respectively. The isotropic coupling constant is smaller than those generally observed^{19,20} for phosphoranyl radicals (R_4P^*) but is considerably larger than those measured^{6,21} for phosphinyl

TABLE 5: EPR Coupling Constants (MHz) and Spin Densities for Radicals A1 and A2

radical		anisotropic coupling			A_{iso}	ρ_s	ρ_p	$\Sigma\rho$
		τ_1	τ_2	τ_3				
A1	^{31}P	364	-175	-190	1171	0.09	0.497	0.587
	^1H	2.7	0.7	-3.3	44			
	^{13}C	3.3	0.3	-3.6	46	0.012	0.015	0.027
A2	^{31}P	364	-178	-186	1170	0.09	0.496	0.586
	^1H	5.6	1.7	-7.3	43			
	^{13}C	4.0	1.0	-5.0	47	0.012	0.019	0.031

species R_2P^* . Previous studies on phosphoniumyl radicals^{6,17,22} have shown that, for this species, the ^{31}P — A_{iso} and ^{31}P — τ_{\parallel} values range from 660 to 1450 and from 420 to 580 MHz, respectively. The EPR parameters shown in Table 5 for radical A are therefore consistent with the trapping of a R_3P^+ radical and we will try to identify this species more precisely.

The fact that the ^{31}P and ^{13}C coupling measured for A1 are almost identical with those measured for A2 implies that the phosphorus ligands are probably the same in A1 and in A2. Since deuteration of the phosphalkene bond has an effect on the spectrum of A2 but not on that of A1, a R_2PH^+ structure does not seem plausible. As shown by the ^{13}C coupling, in both radicals the original phosphalkene carbon remains bound to the phosphorus atom and is characterized by a total spin density of ~0.03 (Table 5); however, the coupling with the original phosphalkene proton is observed for A2 but not for A1, suggesting that the main difference between these two species lies in the orientation of this C—H bond with respect to the phosphorus orbital containing the unpaired electron.

These observations can be rationalized by the radiation mechanism shown in Figure 6. During its deactivation the radiolytically oxidized molecule 1^+ undergoes a homolytic scission of a C—H bond of a *tert*-butyl group located in the ortho position from the phosphalkene moiety. The leaving hydrogen atom adds to the phosphalkene carbon and the resulting RCH_2^* radical forms a bond with the phosphorus atom (see Figure 6). It appears from the experimental results that this intramolecular cyclization can give rise to two conformations A1 and A2 which probably differ in their dihedral angle α formed by the phosphorus $3p_z$ orbital and the C—H bond (Figure 7).

To verify to what extent the above interpretation of the ESR spectra is in accord with the predictions of *ab initio* calculations, we compare the experimental parameters given in Tables 1 and 2 with those predicted for H_3P^+ , $(\text{CH}_3)_3\text{P}^+$, and $\text{H}_2\text{P}^+\text{CH}_3$. As shown in Figure 4 and in Table 3, the various hyperfine couplings of the two former species are strongly dependent upon the pyramidity of the radical. As expected, the increase of the pyramidity angle ξ (Figure 3a) is accompanied by the following properties: (1) an increase in the isotropic ^{31}P coupling constant (increase of the phosphorus s character, Figure 4) and a decrease in the dipolar ^{31}P coupling (Table 3), (2) an increase in the isotropic ^1H coupling for PH_3^+ which is negative for the planar structure (spin polarization), vanishes for $\xi = 102^\circ$ and, then, becomes positive (Figure 4), and (3) an increase in the isotropic ^{13}C coupling of $(\text{CH}_3)_3\text{P}^+$ whose sign changes for $\xi = 98^\circ$ (Figure 4). The dependence of the energy and of the proton isotropic couplings upon the rotation of the methyl group around the P—C bond are shown in Figure 5 for $\text{H}_2\text{P}^+\text{CH}_3$. The methyl ^1H isotropic coupling is very sensitive to the α dihedral angle (Figure 3b): it ranges from -0.4 to 64 MHz while the maximum eigenvalue of the anisotropic coupling lies between 5 and 10 MHz. The α dependence of the isotropic coupling of the methyl protons in $\text{H}_2\text{P}^+\text{CH}_3$ is a pertinent illustration of the effect of the pyramidity of a radical on the

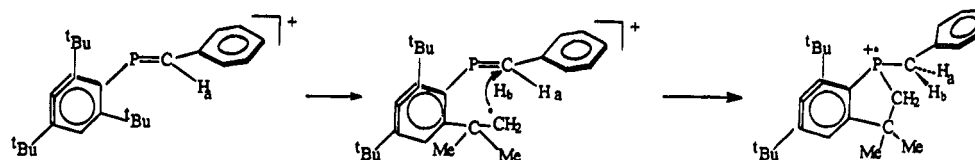


Figure 6. Proposed mechanism for the formation of the phosphoniumyl radical cations.

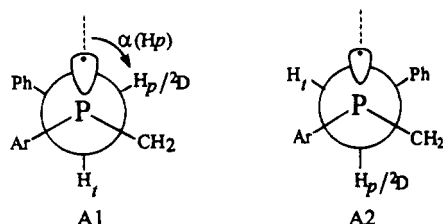


Figure 7. Conformation of the phosphoniumyl radical cations A1 and A2. (H_p represents the hydrogen atom of the parent phosphalkene moiety, it is replaced by a deuterium atom in $^2D-1$, H_t results from the homolytic scission of a C—H bond of a *tert*-butyl group in the parent molecule).

isotropic coupling of a β -proton. For $H_2P^{+}CH_3$ this dependence is quite different from that observed for a planar $CH_3CR_2^{\bullet}$ radical: the isotropic proton coupling does not follow the usual $(A + B \cos^2 \alpha)$ rule and the corresponding curve does not exhibit any π -periodicity but verifies the relation $A_{iso}(\pi - \alpha) = A_{iso}(\pi + \alpha)$: (see the reference proton H_a of Figure 5). As shown in this figure, the minimum energy is obtained when the α dihedral angle of a proton is equal to 180° ; this orientation of the proton corresponds to its maximum isotropic coupling constant and the calculated barrier to the rotation of the methyl group is very low ($1.17 \text{ kcal mol}^{-1}$). In accord with previous calculations,^{13–16} the “staggered” conformation was also found to correspond to the minimum energy conformation for $(CH_3)_3P^{+}$.

The presence of the benzene substituent for the phosphoniumyl radicals trapped in the crystal of **1** certainly increases the height of the energy barrier to the rotation of the CH_2R group. The resulting stabilization of the staggered conformation is probably the cause of the distinction between the species A1 and A2: the addition of the hydrogen atom to the phosphalkene carbon is accompanied by a reorientation of the C—phenyl bond which can make an α angle of $+60^\circ$ or -60° (Figure 7). As shown by Figure 5, when the dihedral angle α of C— H_a is equal to 180° , the couplings of H_b and H_c are almost zero. For the species A1, the $\alpha = 180^\circ$ position is then occupied by the hydrogen atom issuing from the *tert*-butyl group (large coupling which is not affected by the presence of deuterium in *D-1*). For A2, this position is occupied by the original phosphalkene hydrogen atom (large coupling which disappears for *D-1*).

The ^{31}P and 1H hyperfine interactions calculated for the optimized structure of $(CH_3)_3P^{+}$ (^{31}P : $A_{iso} = 1043 \text{ MHz}$, $\tau_{||} = 548 \text{ MHz}$, 1H_a : $A_{iso} = 54 \text{ MHz}$; 1H_b and 1H_c : $A_{iso} = 3.4 \text{ MHz}$) are quite comparable with the experimental values obtained with the species A1 and A2, the ^{13}C isotropic constant ($A_{iso} = 10 \text{ MHz}$) is however significantly smaller than the values reported in Table 5. We calculated, therefore, the hyperfine coupling for the phosphoniumyl radical **2** whose structure is more similar to that proposed for radicals A1 and A2: in this phosphoniumyl radical the phosphorus is incorporated in a five-membered ring containing a C=C bond. The coupling constants calculated after a total optimization of the geometry of this molecule are shown in Table 4. Although the isotropic phosphorus coupling is now around 925 MHz , the ^{31}P and ^{13}C couplings are in reasonable accord with the experimental results, and the fact that only one of the methylene protons leads to a large coupling totally agrees with the spectra described above. A discrepancy arises only

from the large coupling predicted for one of the two methylene protons of the ring and which was never observed on our spectra. It is possible that the conformation of the five-membered ring calculated by *ab initio* is somewhat different from that adopted by the real molecule whose C=C bond is in fact a bond of a benzene moiety. To test the sensitivity of the hyperfine coupling to the conformation of the cyclopentene ring, we slightly altered the conformation of this ring (see Results), and as reported in Table 4, this deformation led to a drastic decrease of the coupling of the protons of the cycle whereas the other couplings of the P— CH_3 fragment were only slightly affected.

It is worthwhile comparing the structure of the R_3P^{+} radicals discussed in this study with that of the well-known PO_3^{2-} species. The calculated atomic charges reported above (see Results) show that PO_3^{2-} can be considered as a phosphoniumyl radical R_3P^{+} where R represents the ligand O^- . Several experimental^{23–27} and theoretical²⁸ studies have been devoted to PO_3^{2-} ; in particular it has been noticed²⁵ that the ^{31}P couplings of this radical are quite sensitive to the nature of the host matrix and, for example, A_{iso} ranges from 1550 MHz ²⁴ (in $(NH_4)_2PO_3F \cdot H_2O$) to 2104 MHz ²⁶ (in $(NH_4)_2H_2P_2O_6$) and $\tau_{||}$ ranges from 282 MHz ²⁷ (in $Na_2DPO_3 \cdot 5D_2O$) to 334 MHz ²⁹ (in $MeOPO_3 \cdot Mg$). Such environmental effects are not, of course, taken into account in our *ab initio* calculations; the optimized structures show that isolated H_3P^{+} and $(CH_3)_3P^{+}$ are slightly more pyramidal ($\xi = \text{ca. } 106^\circ$) than the isolated PO_3^{2-} species ($\xi = \text{ca. } 104^\circ$), whereas single crystal EPR studies^{23,27} ($Na_2HPO_3 \cdot 5H_2O$ and $Na_2DPO_3 \cdot 5D_2O$ matrices) on this last radical had led to a ξ angle close to 110° .

Concluding Remarks

Since pioneering studies that have shown that dicoordinated trivalent phosphorus species can be stabilized by substituents bearing cumbersome moieties (e.g., *tert*-butyl groups), these compounds have been extensively used, especially in coordination chemistry. The phosphorus-containing double bond is however very reactive to radicals and a homolytic scission on the protective group easily leads to a cyclization of the molecule. The present study indicates that a similar reaction can occur in oxidative conditions and, indeed, a cyclic phosphoniumyl radical cation could be trapped as a reaction intermediate in the solid state. As shown by *ab initio* calculations, ^{31}P , ^{13}C , and 1H hyperfine interactions are particularly appropriate for revealing the geometry of phosphoniumyl radicals $R_2P^{+}CH_2R$.

Acknowledgment. The financial support of the Swiss National Research Fund is gratefully acknowledged.

References and Notes

- (1) Appel, R.; Knoll, F.; Ruppert, I. *Angew. Chem., Int. Ed. Engl.* **1981**, *20*, 731.
- (2) Yoshifuji, M.; Shima, I.; Inamoto, N. J.; Hirota K.; Higuchi, T. *J. Am. Chem. Soc.* **1981**, *103*, 4587.
- (3) Cetinkaya, B.; Hudson, A.; Lappert M.; Goldwhite, H. *J. Chem. Soc., Chem. Commun.* **1982**, 609.
- (4) Cattani-Lorente, M.; Geoffroy, M. *J. Chem. Phys.* **1989**, *91*, 1498
- (5) Bhat, S. N.; Berclaz, T.; Jouaiti, A.; Geoffroy, M. *Helv. Chim. Acta* **1994**, *77*, 372.

- (6) Tordo, P. In *The Chemistry of Organophosphorus Compounds*; Patai, P., Hartley, F., Eds.; J. Wiley: New York, 1990; Vol. 1, p 437.
- (7) Palau, C.; Berchadsky, Y.; Chaliar, F.; Finet, J. P.; Gronchi, G.; Tordo, P. *J. Phys. Chem.* **1995**, *99*, 158.
- (8) Yoshifuji, M.; Toyota, K.; Inamoto, N. *Tetrahedron Lett.* **1985**, *26*, 1727.
- (9) Appel, R.; Menzel, J.; Knoch, F.; Volz, P. *Z. Anorg. Allg. Chem.* **1986**, *534*, 100.
- (10) Iwasaki, M. *J. Magn. Reson.* **1974**, *16*, 417.
- (11) Frisch, F. M.; Head-Gordon, M.; Trucks, G. W.; Foresman, J. B.; Schlegel, H. B.; Raghavachari, K.; Robb, M.; Binkley, J. S.; Gonzalez, C.; Defrees, D. J.; Fox, D. J.; Whiteside, R. A.; Seeger, R.; Melius, C. F.; Baker, J.; Martin, R. L.; Kahn, L. R.; Stewart, J. J. P.; Topiol, S.; Pople, J. *Gaussian 90*; Gaussian, Inc.: Pittsburgh, PA, 1990.
- (12) Frisch, M. J.; Trucks, G. W.; Schlegel, H. B.; Gill, P. M. V.; Johnson, B. G.; Wong, M. W.; M.; Foresman, J. B.; Robb, M. A.; Head-Gordon, M.; Replogle, E. S.; Gomperts, R.; Andres, J. L.; ; Raghavachari, K.; Binkley, J. S.; Gonzalez, C.; Martin, R. L.; Fox, D. J.; Defrees, D. J.; Baker, J.; Stewart, J. J. P.; Pople, J. *Gaussian 92/DFT, Revision G.2*, Gaussian Inc.: Pittsburgh, PA, 1993.
- (13) Carmichel, I. *J. Phys. Chem.* **1985**, *89*, 4727.
- (14) Carmichel, I. *Inorg. Chim. Acta* **1986**, *117*, 75.
- (15) Janssen, R. A. J.; Aagaard, O. M.; Cabbolet, M. J. T. F.; de Waal, B. F. M. *J. Phys. Chem.* **1991**, *95*, 9256.
- (16) Cramer, C. J.; Lim, M. H. *J. Phys. Chem.* **1994**, *98*, 5024.
- (17) Symons, M. C. R. and McConnachie G. D. G. *J. Chem. Soc., Chem. Commun.* **1982**, 851.
- (18) Morton, J. R.; Preston, K. F. *J. Magn. Reson.* **1978**, *30*, 577.
- (19) Hammerlink, J. H. H.; Schipper, P.; Buck, H. M. *J. Am. Chem. Soc.* **1983**, *105*, 385.
- (20) Berclaz, T.; Geoffroy, M.; Lucken, E. A. C. *Chem. Phys. Lett.* **1975**, *36*, 677.
- (21) Geoffroy, M.; Lucken, E. A. C.; Mazeline, C. *Mol. Phys.* **1974**, *28*, 839.
- (22) Berclaz, T.; Geoffroy, M. *Mol. Phys.* **1975**, *30*, 549.
- (23) Horsfield, A.; Morton, J. R.; Whiffen, D. H. *Mol. Phys.* **1961**, *4*, 475.
- (24) Herring, F. G.; Hwang, J. H.; Lin, W. C.; McDowell, C. A. *J. Phys. Chem.* **1966**, *70*, 2487.
- (25) Symons, M. C. R. *J. Chem. Soc. A* **1970**, 1998.
- (26) Morton, J. R. *Mol. Phys.* **1963**, *24*, 193.
- (27) Schlick, S.; Silver, B. L.; Luz, Z. *J. Chem. Phys.* **1970**, *52*, 1232.
- (28) Weber, J.; Cornioley Y.; Geoffroy, M. *Chem. Phys. Lett.* **1983**, *96*, 636.
- (29) Nelson, D.; Symons, M. C. R. *J. Chem. Soc., Perkin Trans. 2* **1977**, 286.

JP9516708